ACS PHYSICAL CHEMISTRY Au
AN OPEN ACCESS JOURNAL OF THE AMERICAN CHEMICAL SOCIETY

pubs.acs.org/physchemau

Article

Dual Singlet Excited-State Quenching Mechanisms in an Artificial Caroteno-Phthalocyanine Light Harvesting Antenna

Janneke Ravensbergen, Smitha Pillai, Dalvin D. Méndez-Hernández, Raoul N. Frese, Rienk van Grondelle, Devens Gust, Thomas A. Moore, Ana L. Moore, and John T. M. Kennis*

Cite This: ACS Phys. Chem Au 2022, 2, 59–67

Read Online

ACCESS | Metrics & More | Article Recommendations | Supporting Information

ABSTRACT: Under excess illumination, photosystem II of plants dissipates excess energy through the quenching of chlorophyll fluorescence in the light harvesting antenna. Various models involving chlorophyll quenching by carotenoids have been proposed, including (i) direct energy transfer from chlorophyll to the low-lying optically forbidden carotenoid S_1 state, (ii) formation of a collective quenched chlorophyll−carotenoid S_1 excitonic state, (iii) chlorophyll−carotenoid charge separation and recombination, and (iv) chlorophyll−chlorophyll charge separation and recombination. In previous work, the first three processes were mimicked in model systems: in a Zn-phthalocyanine−carotenoid dyad with an amide linker, direct energy transfer was observed by femtosecond transient absorption spectroscopy, whereas in a Zn-phthalocyanine−carotenoid dyad with an amine linker excitonic quenching was demonstrated. Here, we present a transient absorption spectroscopic study on a Zn-phthalocyanine−carotenoid dyad with a phenylene linker. We observe that two quenching phases of the phthalocyanine excited state exist at 77 and 213 ps in addition to an unquenched phase at 2.7 ns. Within our instrument response of ∼100 fs, carotenoid S_1 features rise which point at an excitonic quenching mechanism. Strikingly, we observe an additional rise of carotenoid S_1 features at 3.6 ps, which shows that a direct energy transfer mechanism in an inverted kinetics regime is also in effect. We assign the 77 ps decay component to excitonic quenching and the 3.6 ps/213 ps rise and decay components to direct energy transfer. Our results indicate that dual quenching mechanisms may be active in the same molecular system, in addition to an unquenched fraction. Computational chemistry results indicate the presence of multiple conformers where one of the dihedral angles of the phenylene linker assumes distinct values. We propose that the parallel quenching pathways and the unquenched fraction result from such conformational subpopulations. Our results suggest that it is possible to switch between different regimes of quenching and nonquenching through a conformational change on the same molecule, offering insights into potential mechanisms used in biological photosynthesis to adapt to light intensity changes on fast time scales.

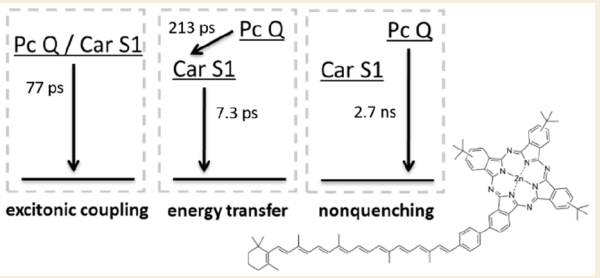

KEYWORDS: *photosynthetic light harvesting, artificial light harvesting dyad, energy transfer, excitonic coupling, nonphotochemical quenching, excess energy dissipation, carotenoid, phthalocyanine, optically forbidden state, ultrafast spectroscopy*

INTRODUCTION

Photosynthetic organisms display a set of photoprotection mechanisms known as nonphotochemical quenching (NPQ).[1,2] NPQ protects the photosynthetic apparatus from photodamage but limits the energy conversion efficiency, as a large portion of solar irradiance is dissipated to heat. Controlling the kinetics of NPQ is one of the main strategies to increase biomass production by photosynthetic organisms.[3] Intense research is focused on understanding the mechanisms of NPQ, and large differences have been found between classes of photosynthetic organisms.[4] To date, several types of mechanisms have been reported, referred to as qE, qI, qT, qZ, and qH.[5−7] In qE, singlet excitations in the light harvesting antenna are dissipated as heat before reaching the reaction center. qE is triggered by acidification of the luminal side of the photosynthetic membrane and is rapidly reversible. During qE, lumen acidification is sensed by the PsbS protein[8] through two active glutamates[9] that protonate upon acidification, triggering a conformational change of PsbS,[10,11] which in turn causes LHCII to assume a quenched conformation.[12] Several molecular mechanisms were discussed for singlet excited-state quenching in oxygenic photosynthesis: (i) Chlorophyll to carotenoid energy transfer, followed by carotenoid internal conversion;[13−21] (ii) chlorophyll−carotenoid charge transfer and subsequent recombination to the ground state;[22,23] (iii)

Received: May 26, 2021
Revised: September 29, 2021
Accepted: September 29, 2021
Published: October 14, 2021

chlorophyll−chlorophyll charge transfer and recombination;[24] (iv) chlorophyll−carotenoid excitonic coupling and internal conversion;[25] and direct pH sensing in the light harvesting complex[26,27] Such mechanisms may occur simultaneously in vivo, such as energy transfer and charge transfer.[28]

Important mechanistic insights into NPQ and the role of carotenoids therein were obtained from studies on artificial light harvesting antennas, in particular phthalocyanine−carotenoid dyads and triads.[21,29−34] In such artificial systems, interactions between tetrapyrroles and carotenoids can be studied isolated from the complexity of its biological environment. Even if the involved pigments (chlorophyll and xanthophyll in oxygenic photosynthesis versus phthalocyanine (Pc) and carotenoid (Car) in dyads and triads) are not identical, they are sufficiently similar to make a meaningful comparison. More than a decade ago, Berera and co-workers were the first to demonstrate that efficient energy transfer from a tetrapyrrole to the low-lying, optically forbidden carotenoid S_1 state was feasible in a dyad where Pc and Car were connected through an amide linker. The directionality of the energy flow was found to strongly depend on conjugation length of the carotenoid, with a change of only one single conjugated double bond turning the carotenoid S_1 state from energy donor into energy acceptor.[30,35] In that work, significantly shortened singlet excited state lifetimes of the tetrapyrrole of down to 30 ps were observed.[30] That work served as a basis for the identification of a similar mechanism in Light Harvesting Complex II (LHCII) aggregates, where Lutein 1 was identified as a quencher of Chl *a* excited states through energy transfer to its optically forbidden S_1 state.[14] Subsequently, Kloz et al. demonstrated an additional quenching model in a similar dyad with an amine linker: in that system, a shared Pc−Car electronic excited state was observed immediately after excitation of the Pc, which was interpreted as arising from excitonic coupling between the Pc Q state and the optically forbidden carotenoid S_1 state, resulting in similarly shorted lifetimes.[31] The results and interpretation of this work were later confirmed by Polli and co-workers.[34] The potential role of electron transfer between tetrapyrroles and carotenoids for NPQ processes[22,23] was addressed in a number of dyads and triads dissolved in polar solvents.[29,31,33,36]

The linker between the carotenoid and tetrapyrrole can have an effect by partitioning in the energy transfer mechanism, in modulating the distance and electronic coupling, and by influencing the relative orientation of the two chromophores.[33,37,38] Here, we report that the same caroteno-phthalocyanine dyad with a phenylene linker can undergo quenching by energy transfer, quenching by excitonic coupling, and nonquenching. We propose the coexistence of these three regimes is caused by conformational variation. Such a conformational effect suggests a switching mechanism that is potentially used in biological photosynthesis to adapt to light intensity changes on fast time scales.

The dyad (Figure 1) consists of a carotenoid linked to a Zn-phthalocyanine by a phenylene linker. The carotenoid has nine double bonds in the polyene chain and an additional double bond in the β-ionone ring and an elongation of the conjugated system into the linker moiety by a phenylene group. The lifetime of its optically forbidden S_1 state, 7.6 ps, is similar to that of lutein and zeaxanthin: in fact, it is somewhat shorter, indicating that its S_1 energy level likely is slightly lower than that of Lut and Zea.

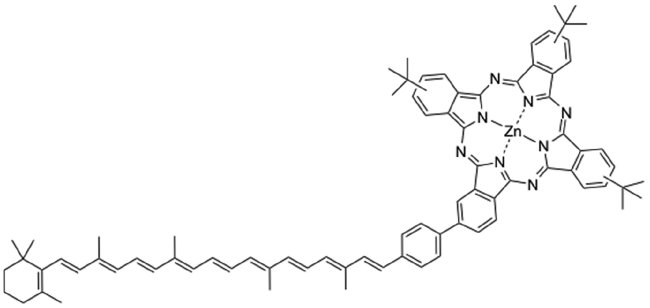

Figure 1. Structure of the caroteno-phthalocyanine dyad.

We compare the dyad with a zinc-tetra-*tert*-butyl-phthalocyanine (Figure S1). A study of the carotenoid part of the dyad has been reported previously.[39] Transient absorption spectroscopy was carried out as described previously.[21] For details on the synthesis and the spectroscopic analysis method, refer to the Supporting Information (SI). In the following, we will refer to the investigated caroteno-phthalocyanine dyad as "dyad" and the reference Zn-phthalocyanine as "Pc-ref". The phthalocyanine and carotenoid parts of the dyad will be called "Pc" and "Car", respectively.

RESULTS AND DISCUSSION

The absorption spectra of the dyad and Pc-ref in toluene are shown and in Figure 2. The absorption spectrum of Pc-ref (red line) agrees with previously reported spectra of zinc-phthalocyanines in the monomeric form.[36] The Q-band (S_0−S_1 transition) has a maximum at 677 nm and vibronic progression bands at 648 and 611 nm. The Soret band (S_0−S_2 transition) has a maximum at 349 nm. The absorption spectrum of the dyad contains the spectral features of Pc-ref reported here and 7′-apo-7-(4-tolyl)-β-carotene (carotenoid reference including the phenyl ring) reported by Berera et al.,[30] but it differs in three respects from the sum of these spectra. First, the carotenoid vibronic bands are less sharp, resulting from the influence of the phthalocyanine on the carotenoid moiety. Second, the absorption features are red-shifted with respect to the references, due to the extension of the conjugated system. The Q-band is red-shifted by 7 to 685 nm. Third, the Q-band in the dyad is broader: 26 nm at half height, compared to 17 nm for Pc-ref. We assign the broadening of the Q-band to the heterogeneity in the sample from different conformations of the dyad. We can safely exclude aggregation as a source of Q-band broadening, because

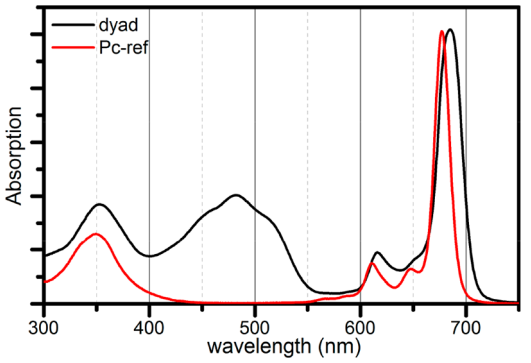

Figure 2. Absorbance spectra of the dyad and Pc-ref in toluene, normalized at the absorbance maximum of the Q-band.

https://doi.org/10.1021/acsphyschemau.1c00008
ACS Phys. Chem Au 2022, 2, 59−67

the spectrum does not resemble the absorption spectrum reported for aggregated Zn-phthalocyanine derivatives.[36]

To assess the photophysics of the dyad and compare the quenching mechanisms with previously studied systems, Pc-ref and dyad were studied by transient absorption spectroscopy. Global analysis of the transient absorption data was performed using the Glotaran program.[40,41] In global analysis, all wavelengths are analyzed simultaneously using a sequentially interconverting model 1 → 2 → 3 → ... Here the numbers indicate evolution associated difference spectra (EADS) that interconvert with successive monoexponential decay rates, each of which can be regarded as the lifetime of each EADS. Data from experiments in the visible and near-IR were fitted simultaneously. The EADS that follow from the sequential analysis are visualizations of the evolution of the (excited) states of the system and usually represent a mixture of molecular species. This sequential analysis is mathematically equivalent to a parallel (sum-of-exponentials) analysis and the time constants that follow from the analysis apply to both.[42] The parallel decay scheme produces decay associated difference spectra (DADS). For a more detailed description of global analysis, we refer to the paper by van Stokkum et al.[40]

Transient absorption spectroscopy data of Pc-ref was globally analyzed, and the data is shown in Figure 3. The fitted kinetics are shown in Figure S2. Five components with time constants of 50 fs (fixed), 192 fs, 2.3 ps, and 3.0 ns and a nondecaying component were needed for a sufficient fit of the data. The first, with a fixed time constant of 50 fs, includes mainly time-zero artifacts and is not shown. The second EADS (black line, 192 fs) has a minimum at 679 nm. This band originates from the ground state bleach (GSB) of the Q-band absorption at 677 nm and stimulated emission (SE) at longer wavelengths. Only one maximum can be detected for these two contributions, in agreement with the small Stokes shift of 4 nm reported for Zn-phthalocyanine in toluene.[36] The minima at 651 and 611 nm originate from bleaching of the vibronic progressions of the Q-band. The GSB and SE overlap with a broad excited state absorption (ESA) feature that spans the visible and near-IR probed range. The changes in the 192 fs and 2.3 ps processes are small: the 192 fs and 2.3 ps DADS (black and red), that show the spectral changes on these time scales, consist of band-shift-like patterns. We attribute these time scales to two phases of solvation.[43] In the 3.0 ns EADS, assigned to the relaxed excited state, the GSB/SE band peaks at 681 nm. The 3.0 ns DADS (blue) shows a loss of ESA, GSB, and SE. We assign this time scale to the decay of the Pc Q state, partly into the triplet state and partly into the ground state. The triplet ΔA spectrum of Pc-ref is given in the last EADS (green), which is not decaying on the 3.5 ns time scale of our experiment. The triplet spectrum contains a single absorption band with a maximum at 505 nm and Q-band GSB, including the vibronic progressions. Compared to the singlet spectrum, the main band has a smaller amplitude at the low energy side, due to the loss of SE upon intersystem crossing. The results for Pc-ref in toluene reported here agree well with the transient absorption spectroscopy results of Zn-phthalocyanine in DMSO reported by Savolainen et al.[43]

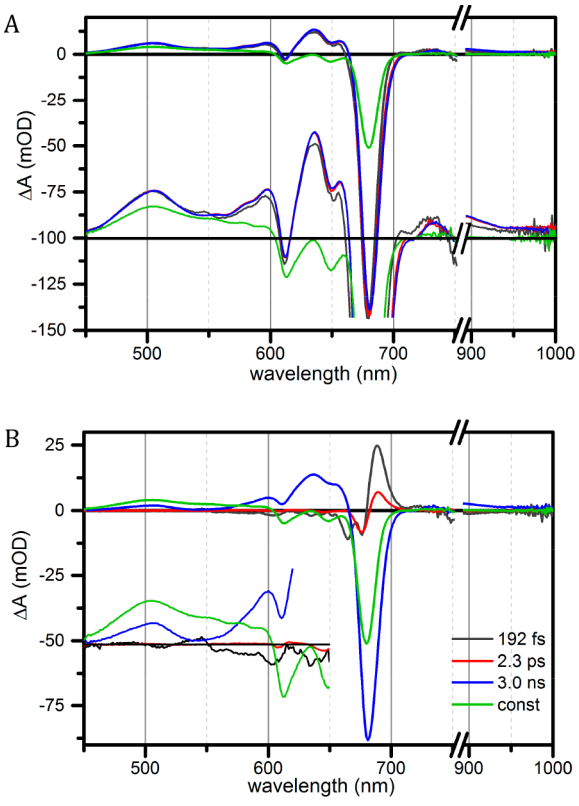

Figure 3. (A) Evolution associated difference spectra (EADS) and (B) decay associated difference spectra (DADS) resulting from global analysis of Pc-ref in toluene upon 670 nm excitation. The lower parts in each panel represent an expansion of the vertical axis by a factor of 5 to facilitate inspection of the ESA region between 460 and 650 nm.

For the dyad, upon excitation at 670 nm, the photophysics is more complex than that in Pc-ref and seven components were needed for a sufficient fit of the transient absorption data: 50 fs (fixed), 348 fs, 3.6 ps, 77 ps, 213 ps, and 2.7 ns and a component that does not decay on the 3.5 ns time scale of our experiment. The EADS resulting from global analysis are presented in Figure 4A, and the DADS are presented in Figure 4B. The time traces are shown in Figure S3. The first EADS with a fixed time constant of 50 fs includes mainly time-zero artifacts, similar to those observed in Pc-ref and is not shown. The subsequent EADS have as the most prominent feature a negative band at 690 nm, with a shoulder at the high energy side, assigned to the stimulated emission and ground state bleach of the Pc moiety, respectively. At wavelengths shorter than 670 nm, excited-state absorption (ESA) is observed, superimposed on a bleach of the Pc vibronic band at 615 nm. The final, nondecaying EADS does not show the stimulated emission and is assigned to a triplet state (vide infra). The most obvious difference with the Pc-ref dynamics is the shortened singlet excited-state lifetime of the dyad: the decay occurs with time constants of 77 ps (blue to green evolution), 213 ps (green to magenta evolution), and 2.7 ns (magenta to cyan evolution). The three distinct PC excited-state lifetimes of 77 ps, 213 ps, and 2.7 ns are demonstrated more clearly in the DADS, where loss of Pc bleach/stimulated emission around 690 nm is clearly observed in each of these components (we recall here that sequential analysis and parallel, sum-of-exponentials analysis are mathematically equivalent).[42] We conclude that the majority of dyads are significantly quenched with respect to Pc-ref (77 and 213 ps components), while a minor fraction has a lifetime that is essentially identical to that of Pc-ref (2.7 ns component). This observation demonstrates that structural heterogeneity exists in the dyad, because if there would be only one structural conformer, a single-exponential excited-state decay would be

https://doi.org/10.1021/acsphyschemau.1c00008
ACS Phys. Chem Au 2022, 2, 59−67

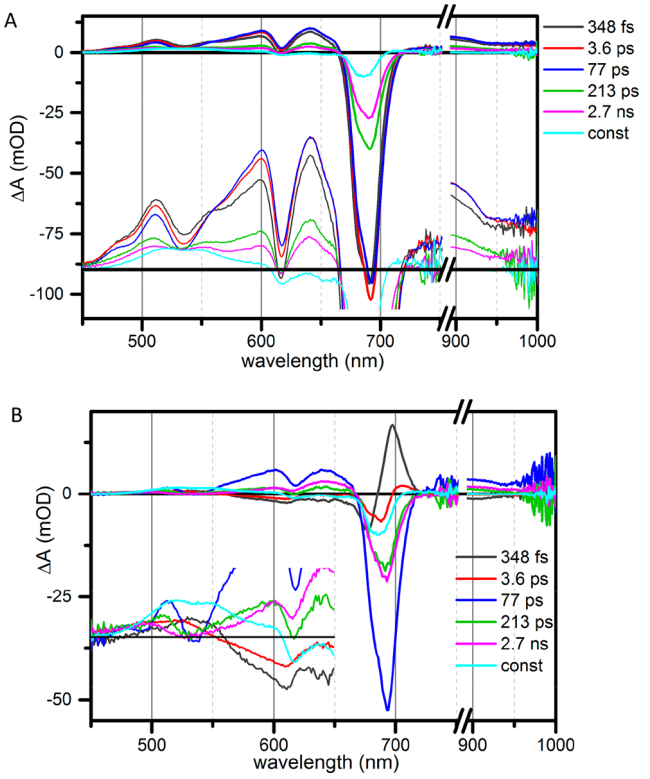

Figure 4. (A) EADS resulting from global analysis of the dyad in toluene upon 670 nm excitation. The lower part represents the same EADS on an expanded vertical scale (5×) to facilitate inspection of the ESA region between 460 and 650 nm. (B) DADS of the same global analysis as in (A) with the lower part the DADS on an expanded vertical scale.

observed. Indeed, computational chemistry calculations indicate the presence of multiple conformers in the dyad (vide infra). In the following, we will identify the mechanisms by which the 77 and 213 ps excited-state decay components are quenched.

Further inspection of the EADS of the Pc-ref and dyad reveals the mechanisms that govern the quenching phenomena in the dyad. A comparison of the 192 and 348 fs EADS of Pc and dyad (Figure 5) shows that significant differences between Pc and dyad exist on this early time scale. Strikingly, the ESA signal at wavelengths shorter than 545 nm is lower for the dyad while the ESA signal between 545 and 615 nm is higher. This

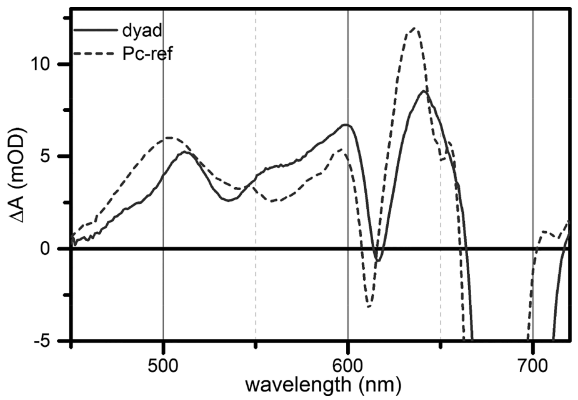

Figure 5. EADS of the dyad (348 fs EADS, solid line) and of Pc-ref (192 fs EADS, dashed line) in toluene upon 670 nm excitation.

phenomenon has been reported previously in carotenoid−hthalocyanine dyads with a phenyl-amine linker and was interpreted as arising from a collective Pc−carotenoid excited state, which arises from excitonic coupling of the phthalocyanine Q state with the S_1 state of carotenoid, where the latter state is only slightly mixed in.[31] Because the mixed-in carotenoid S_1 state has a short lifetime of about 7 ps, the lifetime of the collective Pc−car S_1 state will be significantly shortened with respect to the uncoupled Pc excited state.[31]

To isolate the Car S_1 contribution in the dyad 348 fs EADS, we subtracted the Pc-ref EADS from the dyad EADS after red-shifting the former by 6 nm to account for their shifted ground state absorption (Figure S4, red line). For comparison, we plotted the dyad Car S_1 spectrum that results from direct carotenoid excitation at 530 nm (*vide infra*) (Figure S4, black line) and the Car S_1 spectrum from the model carotenoid reported in ref 39 (Figure S4, blue line). We observe an overall agreement between these spectra with a ground state bleach in the region 450−530 nm and an ESA around 540−600 nm. We note that, at wavelengths longer than 600 nm, in the subtracted dyad spectrum, the effects of the different absorption shapes of the excited Pc Q-band among the two samples start to dominate the difference spectrum.

Upon excitation of this excitonically coupled state, the Car ground state bleach and S_1 absorption appear in the initial spectrum, together with the bleach/stimulated emission of ESA and the excited Pc Q state, of which the latter features dominate. In Figure S5, we present the ΔA spectra (raw data) that are recorded during the instrument response function. Indeed, no changes in spectral shape are found during the rise of signal, showing that it is very unlikely that the appearance of carotenoid features is an effect of fast energy transfer. Hence, we conclude that a quenching mechanism similar to that reported by Kloz et al.[31] is operational in the dyad. As discussed in Kloz et al., because the transition dipole moment of the carotenoid S_1 state is zero, classical exciton theory does not apply to the collective states and redistribution of oscillator strength and spectral shifts do not necessarily occur.

For Pc-ref, two solvation processes were identified at 192 fs and 2.3 ps. Similar time constants were found for the dyad: 348 fs and 3.6 ps (Figure 4). The spectral evolution of both kinetics includes a band shift at the Q-band that can be assigned to solvation, analogous to Pc-ref. However, for the dyad, the 3.6 ps component also includes a spectral change between 450 and 670 nm that was not found in Pc-ref. This process might occur on a slightly different time scale than that of the solvation process, but it could not be resolved separately by the analysis. Because the spectral change is small, its characteristics are optimally inspected from the DADS. Figure 6 shows an overlay of the 3.6 ps DADS of the dyad with the 2.3 ps DADS of Pc. The Pc-ref DADS is spectrally silent at wavelengths shorter than 670 nm; in contrast, the DADS of the dyad displays a positive amplitude below 550 nm and a negative amplitude between 550 and 670 nm. This is a typical signature for a rising contribution of the carotenoid S_1 state,[17,21,30] as can also be seen by inspecting raw transient spectra in Figure S6A. The feature rises on a time scale comparable to that reported time for decay by internal conversion, which is 7.8 ps.[39] The observation that, in the dyad, the solvation time scale (3.6 ps) is clearly longer than that in Pc-ref (2.3 ps) suggests the 3.6 ps component is a weighted average of solvation and Car S_1 population dynamics. It indicates excitation energy transfer from Pc to Car with an "inverted kinetic scheme" in which Car

https://doi.org/10.1021/acsphyschemau.1c00008
ACS Phys. Chem Au 2022, 2, 59−67

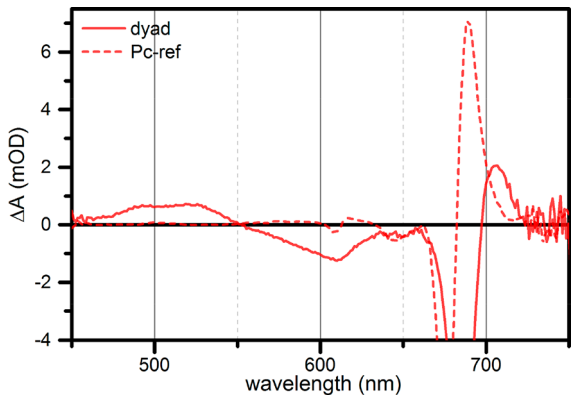

Figure 6. DADS of the dyad (3.6 ps DADS, solid line) and Pc-ref (2.3 ps DADS, dotted line) in toluene upon 670 nm excitation.

is populated on a time scale longer that its decay time.[21,30] As a result, we find a Car S_1 rise signal on the short time scale and a decay superimposed on the spectrum of the Pc energy donor. We conclude that, in addition to the aforementioned excitonic quenching mechanism, a quenching mechanism through Forster-like energy transfer similar to that reported by Berera co-workers[21,30] is in effect in the dyad.

To demonstrate that the 3.6 ps component is required for a proper description of the transient data, we performed global analysis with one component less, resulting in an overall decreased fit quality, presented in Figures S7 and S8.

In the kinetics that follows, the signal evolves with time constants of 77 ps, 213 ps, and 2.7 ns and a time constant beyond the time scale of our experiment (Figure 4). What spectral features decay on which time scales can be seen most clearly from the normalized DADS, as displayed in Figure 7.

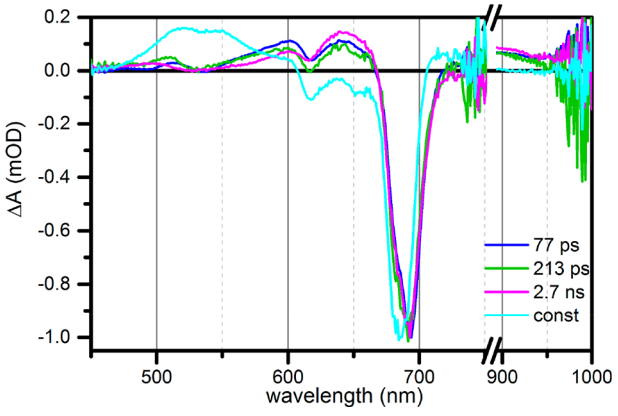

Figure 7. Last four DADS of the dyad in toluene upon 670 nm excitation, normalized at the bleach maximum at 690 nm.

The 2.7 ns (magenta) and nondecaying (cyan) time constants and the corresponding spectra are very similar to the singlet and triplet decay DADS found for Pc. They are ascribed to singlet and triplet decay of a subpopulation with a Pc moiety that is not quenched. We can exclude contamination by free phthalocyanine because a nanosecond lifetime component is also found upon Car S_2 excitation at 530 nm (vide infra), showing that the component arises from the intact dyad.

The 77 and 213 ps time constants have no analogs in the reference components. Compared to the Pc-ref singlet DADS, they have larger amplitudes in the 530−610 nm region, typical of Car S_1 absorption (Figure 7). Given that the 77 ps component has a larger S_1 contribution and represents the largest fractional decay, we propose that this fraction represents the excitonically coupled state as in the work of Kloz et al.[31] Given that the 3.6 ps process represents a very small amplitude, the 213 ps component, which represents a smaller fractional decay, most likely corresponds to an inverted kinetics energy transfer process. This assignment is supported by the relative amplitudes of the 3.6 and 213 ps DADS and the notion that, in inverted kinetics, the maximum transient concentration of the quenching species is the ratio between the slow and fast energy transfer rate constant. Given an internal conversion time constant of 7.3 ps and an energy transfer time constant of 213 ps, this ratio should be approximately 30. The amplitude of the carotenoid S_1 DADS is about 1.2 mOD, and the amplitude of the Pc bleach/stimulated emission is about 20 mOD. With an extinction coefficient of 120 000 M^{-1} cm^{-1} for the carotenoid S_1 state absorption and 280 000 M^{-1} cm^{-1} for the Pc Q state (taking into account that bleach and stimulated emission render the bleach/stimulated emission a factor of 2 higher in the case of a small Stokes shift), one arrives at a transient concentration ratio of about 20, in reasonable agreement with that estimated from the rate constants above.

In the past, Pc quenching by charge separation and recombination, resulting in the transient formation of carotenoid radical cations was observed in a Pc−car dyad with amine linker dissolved in polar solvent (THF). In nonpolar solvent (toluene), no carotenoid radical cations were detected, and quenching was found to proceed via the aforementioned excitonic mixing mechanism.[31] In Pc−car dyads with an amide linker, quenching was found to proceed via direct Pc−Car S_1 energy transfer and become stronger in solvents with higher polarity, which was assigned to the mixing of an intramolecular charge transfer state with the carotenoid S_1 state, mediated by a carbonyl group on the carotenoid conjugated backbone.[39] No carotenoid radical cations were detected in the latter study. Because the solvent in the current study is nonpolar, we do not expect the involvement of carotenoid radical cations in the quenching processes in this study. Accordingly, we did not observe any contribution from a Car radical cation, as can be seen from Figure 4A in the 900−1000 nm region. For a carotenoid radical cation, a distinct broad positive band should be observed around 950−1000 nm, which is not detected, even taking into account that beyond 950 nm the signal becomes noisier.

In a theoretical paper, Valkunas and co-workers[44] attempted to address the quenching mechanism in the dyads described in the Berera[30] and Kloz[31] papers. Although the authors claimed to present a unified model for the quenching, their model has an essential shortcoming in that it failed to reproduce the delocalized excitonic state reported by Kloz et al. In addition, they proposed that the dyad dynamics in the Berera paper did not correspond to inverted kinetics, but described the picosecond dynamics in terms of establishment of a thermal equilibrium between Pc and S_1, which would imply that the carotenoid S_1 would be energetically higher than Pc given that the equilibrium would favor the Pc singlet excited state over the Car S_1 state. This is, however, quite unlikely given that the same dyads do not show any Car S_1−Pc energy transfer upon excitation of the carotenoid S_2 state for carotenoids with 10 and 11 double bonds.[35,45] In addition, the kinetic modeling by Berera et al. reproduced the correct amplitude for the carotenoid S_1 state with respect to that of Pc.[30] Taken

https://doi.org/10.1021/acsphyschemau.1c00008
ACS Phys. Chem Au 2022, 2, 59−67

together, we consider the results presented here and by Berera et al. and Kloz et al. to be robust and correctly interpreted in the respective papers.

The final triplet that is formed shows maxima at 520 and 550 nm. The Pc-ref triplet displayed a maximum at 505 nm. A maximum at 550 nm is typical for the carotenoid triplet. The maximum at 520 nm can be explained by the phthalocyanine triplet ESA being overlapped the with carotenoid bleach at short wavelengths. The final spectrum thus consists of a mixture of carotenoid and phthalocyanine triplets and/or a delocalized triplet state.[46−48]

Transient absorption spectroscopy results for the dyad upon 530 nm excitation are presented in Figures S9 and S10. The elucidated kinetic pathway matches with the findings discussed so far. Interestingly, a Car S* to S_1 evolution process was found, a process that was reported previously by Berera et al. on a different Pc−car dyad.[35] A small fraction of Pc Q decays on a nanosecond time scale, assigned to the nonquenching subpopulation of dyad. This phthalocyanine Q state must originate from energy transfer from Car S_2, confirming that there is a fraction of intact dyad in which Pc Q to Car S_1 energy transfer does not occur.

In the search for possible molecular conformations of the dyad, computational chemistry was used to explore the rotational energy barriers in the ground state for the dihedral angles between the Zn-phthalocyanine and phenylene linker and between the phenylene linker and the carotenoid. The results are shown in Figure S11. We found rotational energy barriers of about 3 and 6 kcal/mol for the two dihedral angles, α and β, respectively. Since the thermal energy at room temperatures is about 0.6 kcal/mol, based on these calculations at least 2 possible ground state conformations are expected to be significantly populated. These conformations differ from each other significantly in terms on the distance and relative orientation between the Zn-phthalocyanine and carotenoid, which is consistent with the multiple quenching mechanisms observed experimentally. Additionally, the potential energy surface wells between the rotational barriers are quite shallow, and thus, multiple conformations within these energy wells are also expected to be populated. We note that in the past, distinct Pc-car conformers were observed in Pc−car triads using NMR spectroscopy and structural modeling.[33]

The presented transient absorption data contains three kinetic pathways that are found to occur in parallel, as illustrated in Scheme 1. As indicated by the computational chemistry results discussed above, multiple conformers are indeed expected with dihedral angle α assuming two distinct conformations. We therefore propose that the parallel pathways are a result of subpopulations of conformers. The strongest coupling is expected for a (close to) planar conformation, in which the conjugated system can be extended throughout the two chromophores, corresponding to conformation 1. The observed excitonically coupled excited state with a 77 ps lifetime is expected to arise from this conformation. If the coupling is substantially decreased, the excited Pc Q state will decay without interaction with the Car S_1 state and will not be quenched. We tentatively assign this unquenched fraction with a 2.7 ns lifetime to conformation 2. The question arises which conformation corresponds to quenching via the Car S_1 state with a 213 ps lifetime. As noted above, the potential energy surface wells between the rotational barriers are quite shallow, which allows for significant twisting of dihedral angles α. Such twisting will decrease the degree of coupling: a diminished coupling leads to more independent excited states in which the Pc Q state may be quenched by excited state energy transfer. We therefore tentatively assign the quenched fraction via energy transfer to a subpopulation of conformer 1 with significantly twisted dihedral angles α. Further computational studies are required to definitively conclude which conformations contribute to each specific mechanism. We also caution that the computational chemistry results were obtained in the gas phase and that specific solvent interactions may affect the conformational structure energy landscape.

Our results on the dyad show that it is possible to switch between different regimes of quenching and nonquenching, presumably through a conformational change on the same molecule. These results suggest that a switching mechanism to adapt to light intensity changes on fast time scales could be possible in natural photosynthesis given certain changes within the protein environment that alter the pigments conformation and orientation.

Scheme 1. Kinetic Pathways Corresponding to the Three Degrees of Coupling between the Two Chromophores Derived from the Data as Discussed in the Text[a]

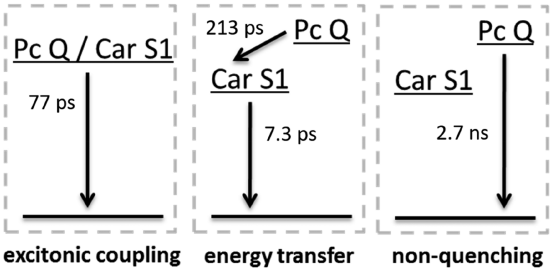

[a]For the energy transfer pathway, the internal conversion time constant of the carotenoid was taken rather than the fitted time constant.

MATERIALS AND METHODS

Dyad Synthesis

The ^{1}HNMR was recorded on a Varian spectrometer at 400 MHz, at 25 °C. The dyad was dissolved in octadeuterotetrahydrofuran (THF-d_8). Mass spectra data was obtained on a matrix-assisted laser desorption/ionization time-of-flight (MALDI-TOF) spectrometer on positive ion mode employing a terthiophene matrix. Ultraviolet−visible ground state absorption spectra were measured on a Shimadzu UV 2100 spectrometer. Chemicals were purchased from Aldrich. All the solvents were obtained from EM Science. The synthesis of 7′-apo-7′-(4-iodophenyl)-β-carotene and Pc-pinacol boronate has been previously reported.[45,49]

Procedure. 7′-Apo-7′-(4-iodophenyl)-β-carotene (14 mg, 0.023 mmol), Pc-pinacol boronate (20 mg, 0.023 mmol), [1,1′ bis-(diphenylphosphino)ferrocene]dichloropalladium(II) (2 mg, 0.003 mmol), potassium acetate (6 mg, 0.063 mmol), were stirred in DMF (3 mL) at 90 °C for 2 h under argon atmosphere. The solution was then allowed to cool to room temperature and the solvent was evaporated under vacuum. The residue was dissolved in dichloromethane and washed with water. The organic layer was dried over anhydrous Na_2SO_4 and evaporated under vacuum. The crude product was purified by column chromatography on silica gel using 10% ethyl acetate in toluene to yield the dyad (16 mg, 57%). ^{1}H NMR (400 MHz, THF-d_8): δ1.04 (6H, s, CH_3-16C and CH_3-17C), 1.46−1.52 (2H, m, CH_2−2C), 1.60−1.69(2H, m, CH_2−3C), (30H, CH_3-19C, CH_3-tBu), 1.95−2.18(11H, m, CH_3-18C, CH_3-20C, CH_3-19′C, CH_2−4C), 2.42(3H, s, CH_3-20′C), 6.05−7.25(14H, m, vinyl H),

https://doi.org/10.1021/acsphyschemau.1c00008
ACS Phys. Chem Au 2022, 2, 59−67

7.50−7.9 (4H, m, Car-1′ 2′, 4′ 5′), 8.16−8.53(3H, m, Pc-H), 9.3−9.78(9H, m, Pc-H). MALDI-TOF-MS *m/z*.: calcd. for $C_{81}H_{84}N_8Zn$ 1232.61, obsd. 1232.78; UV−vis (dichloromethane) 350, 480, 625, 695 nm.

Zinc-tetra-*tert*-butyl-phthalocyanine (Pc-ref) was purchased from Sigma-Aldrich and was purified by chromatography on silica gel with using 500:1 dichloromethane/ethanol. The structure of Pc-ref is given in Figure S1.

Ultrafast Spectroscopy

For transient absorption spectroscopy, the prepared molecules were dissolved in nitrogen-flushed toluene and transferred to a 1 mm path length quartz cuvette. The concentration was set to produce an absorbance of 0.6 at the excitation wavelength of 670 nm. Room-temperature absorption spectra were recorded on a Cary 4000 UV−vis spectrometer.

Ultrafast transient absorption spectroscopy was performed on a setup described earlier.[21,50] In short, the output of an 800 nm, 1 kHz amplified Ti:Sapphire laser system (Coherent Legend) was used to drive an optical parametric amplifier (Coherent OPerA) to produce the excitation pulses. The excitation wavelength was set at 670 nm for Pc-ref and at 530 and 670 nm for the dyad. The pulse energy was set to 100 nJ per pulse and focused to a spot of 400 μm diameter. The probe pulse had a diameter of 200 μm.The probe pulse was created by focusing part of the 800 nm beam on a sapphire plate. For the UV−vis experiments, a 750 nm short-pass filter was used to block the 800 nm fundamental beam. For the near-IR experiments, a 850 nm long pass filter was used to block the 800 nm fundamental beam and second order diffraction. The UV−vis and near-IR experiments were conducted consecutively on the same day.

The pump and probe were focused on the sample and the polarization was set to the magic angle of 54.7°. Absorption difference spectra (ΔA) were calculated by $\Delta A(\lambda) = -\log(I_{pumped})/\log(I_{unpumped})$ for delays up to 3.5 ns. The instrument response function had a width of 100 fs (full width at half-maximum). The spectral chirp was fitted with a third order polynomial.

Global Analysis

Global analysis of the transient absorption data was performed using the program Glotaran.[40,41] In global analysis, all wavelengths are analyzed simultaneously using a sequentially interconverting model 1 → 2 → 3 → ... Here the numbers indicate EADS that interconvert with successive monoexponential decay rates, each of which can be regarded as the lifetime of each EADS. Data from experiments in the visible and near-IR were fitted simultaneously. The EADS that follow from the sequential analysis are visualizations of the evolution of the (excited) states of the system and usually represent a mixture of molecular species. This sequential analysis is mathematically equivalent to a parallel (sum-of-exponentials) analysis and the time constants that follow from the analysis apply to both.[42] The parallel decay scheme produces DADS. For a more detailed description of global analysis we refer to the paper by van Stokkum et al.[40]

Computational Methodology

The hybrid density functional theory functional wB97XD combined with the 6-31G(d) basis set was used to perform two dihedral angle scans of the Zn-phthalocyanine−carotenoid dyad in Gaussian 09. The first dihedral angle scanned was between the Zn-phthalocyanine and phenyl ring and the second between the phenyl ring and the carotenoid. The calculation was done in the gas phase.

■ ASSOCIATED CONTENT

Supporting Information

The Supporting Information is available free of charge at https://pubs.acs.org/doi/10.1021/acsphyschemau.1c00008.

Structure of Pc-ref compound, raw transient spectra, raw kinetics and fits, reconstructed Car S_1 spectrum, EADS, DADS, and kinetics of dyad upon 670 nm excitation with one less component, EADS, DADS, and kinetics of dyad upon 530 nm excitation, computational chemistry structural calculations (PDF)

■ AUTHOR INFORMATION

Corresponding Author

John T. M. Kennis − *Department of Physics and Astronomy, Faculty of Sciences, Vrije Universiteit, 1081 HV Amsterdam, The Netherlands;* orcid.org/0000-0002-3563-2353; Email: j.t.m.kennis@vu.nl

Authors

Janneke Ravensbergen − *Department of Physics and Astronomy, Faculty of Sciences, Vrije Universiteit, 1081 HV Amsterdam, The Netherlands*

Smitha Pillai − *School of Molecular Sciences and Center for Bioenergy and Photosynthesis, Arizona State University, Tempe, Arizona 85287-1605, United States*

Dalvin D. Méndez-Hernández − *University of Puerto Rico at Cayey, Cayey, Puerto Rico 00736*

Raoul N. Frese − *Department of Physics and Astronomy, Faculty of Sciences, Vrije Universiteit, 1081 HV Amsterdam, The Netherlands;* orcid.org/0000-0001-8243-9954

Rienk van Grondelle − *Department of Physics and Astronomy, Faculty of Sciences, Vrije Universiteit, 1081 HV Amsterdam, The Netherlands*

Devens Gust − *School of Molecular Sciences and Center for Bioenergy and Photosynthesis, Arizona State University, Tempe, Arizona 85287-1605, United States;* orcid.org/0000-0003-0550-8498

Thomas A. Moore − *School of Molecular Sciences and Center for Bioenergy and Photosynthesis, Arizona State University, Tempe, Arizona 85287-1605, United States;* orcid.org/0000-0002-1577-7117

Ana L. Moore − *School of Molecular Sciences and Center for Bioenergy and Photosynthesis, Arizona State University, Tempe, Arizona 85287-1605, United States;* orcid.org/0000-0002-6653-9506

Complete contact information is available at: https://pubs.acs.org/10.1021/acsphyschemau.1c00008

Notes

The authors declare no competing financial interest.

■ ACKNOWLEDGMENTS

J.R. was supported by the research programme of BioSolar Cells, cofinanced by the Dutch Ministry of Economic Affairs. J.T.M.K. and J.R. were supported by a VICI grant of the Chemical Sciences council of The Netherlands Organization of Scientific Research (NWO−CW). The synthesis part of this research was supported by the U.S. Department of Energy, Office of Science, Office of Basic Energy Sciences, under Award DE-FG02-03ER15393.

■ ABBREVIATIONS

NPQ: nonphotochemical quenching
qE: quenching of excitation energy
EADS: evolution associated difference spectrum
DADS: decay associated difference spectrum
ESA: excited-state absorption
dyad: caroteno-phthalocyanine dyad in Figure 1
Pc-ref: phthalocyanine reference in Figure S1

Pc: phthalocyanine part of dyad
Car: carotenoid part of dyad

REFERENCES

(1) Rochaix, J.-D. Regulation and Dynamics of the Light-Harvesting System. *Annu. Rev. Plant Biol.* **2014**, *65* (1), 287−309.
(2) Croce, R.; van Amerongen, H. Natural strategies for photosynthetic light harvesting. *Nat. Chem. Biol.* **2014**, *10* (7), 492−501.
(3) Kromdijk, J.; Glowacka, K.; Leonelli, L.; Gabilly, S. T.; Iwai, M.; Niyogi, K. K.; Long, S. P. Improving photosynthesis and crop productivity by accelerating recovery from photoprotection. *Science* **2016**, *354* (6314), 857−861.
(4) Goss, R.; Lepetit, B. Biodiversity of NPQ. *J. Plant Physiol.* **2015**, *172*, 13−32.
(5) de Bianchi, S.; Ballottari, M.; Dall'Osto, L.; Bassi, R. Regulation of plant light harvesting by thermal dissipation of excess energy. *Biochem. Soc. Trans.* **2010**, *38* (2), 651−660.
(6) Nilkens, M.; Kress, E.; Lambrev, P.; Miloslavina, Y.; Muller, M.; Holzwarth, A. R.; Jahns, P. Identification of a slowly inducible zeaxanthin-dependent component of non-photochemical quenching of chlorophyll fluorescence generated under steady-state conditions in Arabidopsis. *Biochim. Biophys. Acta, Bioenerg.* **2010**, *1797* (4), 466−475.
(7) Malnoe, A. Photoinhibition or photoprotection of photosynthesis? Update on the (newly termed) sustained quenching component qH. *Environ. Exp. Bot.* **2018**, *154*, 123−133.
(8) Li, X. P.; Bjorkman, O.; Shih, C.; Grossman, A. R.; Rosenquist, M.; Jansson, S.; Niyogi, K. K. A pigment-binding protein essential for regulation of photosynthetic light harvesting. *Nature* **2000**, *403* (6768), 391−395.
(9) Li, X. P.; Gilmore, A. M.; Caffarri, S.; Bassi, R.; Golan, T.; Kramer, D.; Niyogi, K. K. Regulation of photosynthetic light harvesting involves intrathylakoid lumen pH sensing by the PsbS protein. *J. Biol. Chem.* **2004**, *279* (22), 22866−22874.
(10) Krishnan-Schmieden, M.; Konold, P. E.; Kennis, J. T. M.; Pandit, A. The molecular pH response of the plant light-stress sensor PsbS. *Nat. Commun.* **2021**, *12*, 2291.
(11) Liguori, N.; Campos, S. R. R.; Baptista, A. M.; Croce, R. Molecular Anatomy of Plant Photoprotective Switches: The Sensitivity of PsbS to the Environment, Residue by Residue. *J. Phys. Chem. Lett.* **2019**, *10* (8), 1737−1742.
(12) Nicol, L.; Croce, R. The PsbS protein and low pH are necessary and sufficient to induce quenching in the light-harvesting complex of plants LHCII. *Sci. Rep.* **2021**, *11* (1), 7415.
(13) Frank, H. A.; Cua, A.; Chynwat, V.; Young, A.; Gosztola, D.; Wasielewski, M. R. PHOTOPHYSICS OF THE CAROTENOIDS ASSOCIATED WITH THE XANTHOPHYLL CYCLE IN PHOTOSYNTHESIS. *Photosynth. Res.* **1994**, *41* (3), 389−395.
(14) Ruban, A. V.; Berera, R.; Ilioaia, C.; van Stokkum, I. H. M.; Kennis, J. T. M.; Pascal, A. A.; van Amerongen, H.; Robert, B.; Horton, P.; van Grondelle, R. Identification of a mechanism of photoprotective energy dissipation in higher plants. *Nature* **2007**, *450* (7169), 575−578.
(15) Staleva, H.; Komenda, J.; Shukla, M. K.; Slouf, V.; Kana, R.; Polivka, T.; Sobotka, R. Mechanism of photoprotection in the cyanobacterial ancestor of plant antenna proteins. *Nat. Chem. Biol.* **2015**, *11* (4), 287−U96.
(16) Hontani, Y.; Kloz, M.; Polivka, T.; Shukla, M.; Sobotka, R.; Kennis, J. T. Molecular Origin of Photoprotection in Cyanobacteria Probed by Watermarked Femtosecond Stimulated Raman Spectroscopy. *J. Phys. Chem. Lett.* **2018**, *9*, 1788−1792.
(17) Liguori, N.; Xu, P.; van Stokkum, I. H.; van Oort, B.; Lu, Y.; Karcher, D.; Bock, R.; Croce, R. Different carotenoid conformations have distinct functions in light-harvesting regulation in plants. *Nat. Commun.* **2017**, *8* (1), 1994.
(18) Mascoli, V.; Liguori, N.; Xu, P.; Roy, L. M.; van Stokkum, I. H. M.; Croce, R. Capturing the Quenching Mechanism of Light-Harvesting Complexes of Plants by Zooming in on the Ensemble. *Chem.* **2019**, *5*, 2900−2912.
(19) Van Oort, B.; Roy, L. M.; Xu, P.; Lu, Y.; Karcher, D.; Bock, R.; Croce, R. Revisiting the role of xanthophylls in nonphotochemical quenching. *J. Phys. Chem. Lett.* **2018**, *9* (2), 346−352.
(20) Son, M. J.; Pinnola, A.; Gordon, S. C.; Bassi, R.; Schlau-Cohen, G. S. Observation of dissipative chlorophyll-to-carotenoid energy transfer in light-harvesting complex II in membrane nanodiscs. *Nat. Commun.* **2020**, *11* (1), 1295.
(21) Berera, R.; van Grondelle, R.; Kennis, J. T. M. Ultrafast transient absorption spectroscopy: principles and application to photosynthetic systems. *Photosynth. Res.* **2009**, *101* (2−3), 105−118.
(22) Holt, N. E.; Zigmantas, D.; Valkunas, L.; Li, X.-P.; Niyogi, K. K.; Fleming, G. R. Carotenoid Cation Formation and the Regulation of Photosynthetic Light Harvesting. *Science* **2005**, *307* (5708), 433−436.
(23) Ahn, T. K.; Avenson, T. J.; Ballottari, M.; Cheng, Y. C.; Niyogi, K. K.; Bassi, R.; Fleming, G. R. Architecture of a charge-transfer state regulating light harvesting in a plant antenna protein. *Science* **2008**, *320* (5877), 794−797.
(24) Miloslavina, Y.; Wehner, A.; Lambrev, P. H.; Wientjes, E.; Reus, M.; Garab, G.; Croce, R.; Holzwarth, A. R. Far-red fluorescence: A direct spectroscopic marker for LHCII oligomer formation in non-photochemical quenching. *FEBS Lett.* **2008**, *582* (25−26), 3625−3631.
(25) Bode, S.; Quentmeier, C. C.; Liao, P.-N.; Hafi, N.; Barros, T.; Wilk, L.; Bittner, F.; Walla, P. J. On the regulation of photosynthesis by excitonic interactions between carotenoids and chlorophylls. *Proc. Natl. Acad. Sci. U. S. A.* **2009**, *106* (30), 12311−12316.
(26) Liguori, N.; Roy, L. M.; Opacic, M.; Durand, G.; Croce, R. Regulation of Light Harvesting in the Green Alga Chlamydomonas reinhardtii: The C-Terminus of LHCSR Is the Knob of a Dimmer Switch. *J. Am. Chem. Soc.* **2013**, *135* (49), 18339−18342.
(27) Troiano, J. M.; Perozeni, F.; Moya, R.; Zuliani, L.; Baek, K.; Jin, E.; Cazzaniga, S.; Ballottari, M.; Schlau-Cohen, G. S. Identification of distinct pH- and zeaxanthin-dependent quenching in LHCSR3 from Chlamydomonas reinhardtii. *eLife* **2021**, *10*, e60383.
(28) Park, S.; Steen, C. J.; Lyska, D.; Fischer, A. L.; Endelman, B.; Iwai, M.; Niyogi, K. K.; Fleming, G. R. Chlorophyll-carotenoid excitation energy transfer and charge transfer in Nannochloropsis oceanica for the regulation of photosynthesis. *Proc. Natl. Acad. Sci. U. S. A.* **2019**, *116* (9), 3385−3390.
(29) Kodis, G.; Herrero, C.; Palacios, R.; Mariño-Ochoa, E.; Gould, S.; de la Garza, L.; van Grondelle, R.; Gust, D.; Moore, T. A.; Moore, A. L.; Kennis, J. T. M. Light Harvesting and Photoprotective Functions of Carotenoids in Compact Artificial Photosynthetic Antenna Designs. *J. Phys. Chem. B* **2004**, *108* (1), 414−425.
(30) Berera, R.; Herrero, C.; van Stokkum, I. H. M.; Vengris, M.; Kodis, G.; Palacios, R. E.; van Amerongen, H.; van Grondelle, R.; Gust, D.; Moore, T. A.; Moore, A. L.; Kennis, J. T. M. A simple artificial light-harvesting dyad as a model for excess energy dissipation in oxygenic photosynthesis. *Proc. Natl. Acad. Sci. U. S. A.* **2006**, *103* (14), 5343−5348.
(31) Kloz, M.; Pillai, S.; Kodis, G.; Gust, D.; Moore, T. A.; Moore, A. L.; van Grondelle, R.; Kennis, J. T. M. Carotenoid Photoprotection in Artificial Photosynthetic Antennas. *J. Am. Chem. Soc.* **2011**, *133* (18), 7007−7015.
(32) Liao, P.-N.; Pillai, S.; Kloz, M.; Gust, D.; Moore, A. L.; Moore, T. A.; Kennis, J. T. M.; van Grondelle, R.; Walla, P. J. On the role of excitonic interactions in carotenoid-phthalocyanine dyads and implications for photosynthetic regulation. *Photosynth. Res.* **2012**, *111* (1−2), 237−243.
(33) Palacios, R. E.; Kodis, G.; Herrero, C.; Ochoa, E. M.; Gervaldo, M.; Gould, S. L.; Kennis, J. T. M.; Gust, D.; Moore, T. A.; Moore, A. L. Tetrapyrrole Singlet Excited State Quenching by Carotenoids in an Artificial Photosynthetic Antenna†. *J. Phys. Chem. B* **2006**, *110* (50), 25411−25420.
(34) Maiuri, M.; Snellenburg, J. J.; van Stokkum, I. H. M.; Pillai, S.; Carter, K. W.; Gust, D.; Moore, T. A.; Moore, A. L.; van Grondelle, R.; Cerullo, G.; Polli, D. Ultrafast Energy Transfer and Excited State

https://doi.org/10.1021/acsphyschemau.1c00008
ACS Phys. Chem Au 2022, 2, 59−67

Coupling in an Artificial Photosynthetic Antenna. *J. Phys. Chem. B* **2013**, *117* (46), 14183−14190.
(35) Berera, R.; van Stokkum, I. H. M.; Kodis, G.; Keirstead, A. E.; Pillai, S.; Herrero, C.; Palacios, R. E.; Vengris, M.; van Grondelle, R.; Gust, D.; Moore, T. A.; Moore, A. L.; Kennis, J. T. M. Energy Transfer, Excited-State Deactivation, and Exciplex Formation in Artificial Caroteno-Phthalocyanine Light-Harvesting Antennas†. *J. Phys. Chem. B* **2007**, *111* (24), 6868−6877.
(36) Pillai, S.; Ravensbergen, J.; Antoniuk-Pablant, A.; Sherman, B. D.; van Grondelle, R.; Frese, R. N.; Moore, T. A.; Gust, D.; Moore, A. L.; Kennis, J. T. M. Carotenoids as electron or excited-state energy donors in artificial photosynthesis: an ultrafast investigation of a carotenoporphyrin and a carotenofullerene dyad. *Phys. Chem. Chem. Phys.* **2013**, *15* (13), 4775−4784.
(37) Gust, D.; Moore, T. A.; Moore, A. L.; Devadoss, C.; Liddell, P. A.; Hermant, R.; Nieman, R. A.; Demanche, L. J.; DeGraziano, J. M.; Gouni, I. Triplet and singlet energy transfer in carotene-porphyrin dyads: role of the linkage bonds. *J. Am. Chem. Soc.* **1992**, *114* (10), 3590−3603.
(38) Bensasson, R. V.; Land, E. J.; Moore, A. L.; Crouch, R. L.; Dirks, G.; Moore, T. A.; Gust, D. Mimicry of antenna and photoprotective carotenoid functions by a synthetic carotenoporphyrin. *Nature* **1981**, *290* (5804), 329−332.
(39) Berera, R.; Moore, G. F.; van Stokkum, I. H. M.; Kodis, G.; Liddell, P. A.; Gervaldo, M.; van Grondelle, R.; Kennis, J. T. M.; Gust, D.; Moore, T. A.; Moore, A. L. Charge separation and energy transfer in a caroteno−C60 dyad: photoinduced electron transfer from the carotenoid excited states. *Photochem. Photobiol. Sci.* **2006**, *5* (12), 1142−1149.
(40) van Stokkum, I. H. M.; Larsen, D. S.; van Grondelle, R. Global and target analysis of time-resolved spectra. *Biochim. Biophys. Acta, Bioenerg.* **2004**, *1657* (2), 82−104.
(41) Snellenburg, J. J.; Laptenok, S.; Seger, R.; Mullen, K. M.; Van Stokkum, I. H. M. Glotaran: A Java-Based Graphical User Interface for the R Package TIMP. *J. Stat. Soft.* **2012**, *49* (3), 22.
(42) Toh, K. C.; Stojković, E. A.; van Stokkum, I. H. M.; Moffat, K.; Kennis, J. T. M. Fluorescence quantum yield and photochemistry of bacteriophytochrome constructs. *Phys. Chem. Chem. Phys.* **2011**, *13* (25), 11985−11985.
(43) Savolainen, J.; van der Linden, D.; Dijkhuizen, N.; Herek, J. L. Characterizing the functional dynamics of zinc phthalocyanine from femtoseconds to nanoseconds. *J. Photochem. Photobiol., A* **2008**, *196* (1), 99−105.
(44) Balevicius, V., Jr.; Gelzinis, A.; Abramavicius, D.; Valkunas, L. Excitation Energy Transfer and Quenching in a Heterodimer: Applications to the Carotenoid-Phthalocyanine Dyads. *J. Phys. Chem. B* **2013**, *117* (38), 11031−11041.
(45) Kloz, M.; Pillai, S.; Kodis, G.; Gust, D.; Moore, T. A.; Moore, A. L.; van Grondelle, R.; Kennis, J. T. M. New light-harvesting roles of hot and forbidden carotenoid states in artificial photosynthetic constructs. *Chem. Sci.* **2012**, *3* (6), 2052−2061.
(46) Gall, A.; Berera, R.; Alexandre, M. T.A.; Pascal, A. A.; Bordes, L.; Mendes-Pinto, M. M.; Andrianambinintsoa, S.; Stoitchkova, K. V.; Marin, A.; Valkunas, L.; Horton, P.; Kennis, J. T.M.; van Grondelle, R.; Ruban, A.; Robert, B. Molecular Adaptation of Photoprotection: Triplet States in Light-Harvesting Proteins. *Biophys. J.* **2011**, *101* (4), 934−942.
(47) Bonetti, C.; Alexandre, M. T. A.; van Stokkum, I. H. M.; Hiller, R. G.; Groot, M. L.; van Grondelle, R.; Kennis, J. T. M. Identification of excited-state energy transfer and relaxation pathways in the peridinin−chlorophyll complex: an ultrafast mid-infrared study. *Phys. Chem. Chem. Phys.* **2010**, *12* (32), 9256−9266.
(48) Alexandre, M. T. A.; Luhrs, D. C.; van Stokkum, I. H. M.; Hiller, R.; Groot, M. L.; Kennis, J. T. M.; Van Grondelle, R. Triplet state dynamics in peridinin-chlorophyll-a-protein: A new pathway of photoprotection in LHCs? *Biophys. J.* **2007**, *93* (6), 2118−2128.
(49) Ali, H.; van Lier, J. E. Phthalocyanine-boronates: a synthon for the preparation of molecular assemblies. *Tetrahedron Lett.* **2009**, *50* (3), 337−339.
(50) Bonetti, C.; Stierl, M.; Mathes, T.; van Stokkum, I. H. M.; Mullen, K. M.; Cohen-Stuart, T. A.; van Grondelle, R.; Hegemann, P.; Kennis, J. T. M. The Role of Key Amino Acids in the Photoactivation Pathway of the Synechocystis Slr1694 BLUF Domain. *Biochemistry* **2009**, *48* (48), 11458−11469.

https://doi.org/10.1021/acsphyschemau.1c00008
ACS Phys. Chem Au 2022, 2, 59−67